water

MDPI

Article

Cu(II) Adsorption from Aqueous Solution onto Poly(Acrylic Acid/Chestnut Shell Pigment) Hydrogel

Hui Zhang, Guo-Wei Li, Wei Feng and Zeng-Yu Yao *

Key Laboratory of Forest Resources Conservation and Utilization in the Southwest Mountains of China (Southwest Forestry University), Ministry of Education, Kunming 650224, China
* Correspondence: z-yyao@hotmail.com

Abstract: Powerful adsorbents for heavy-metal removal from wastewater are attractive due to the growing effluent of industries. Developing hydrogels is a current research interest in heavy-metal adsorption from aqueous solutions. We prepared a novel melanin-based hydrogel from renewable chestnut shell pigment and acrylic acid by radical polymerization free from a traditional crosslinker. The synthesized material was characterized by Fourier transform infrared spectroscopy and scanning electron microscope. Its Cu(II)-adsorption performance from the water was evaluated by equilibrium isotherms, kinetics, and thermodynamics. The results indicate that: (1) The dry hydrogel showed a porous structure with a network of interconnected spindle-shaped bars, which makes it feasible to serve as an adsorbent; (2) The kinetic adsorption data followed both the pseudo-first-order and the pseudo-second-order models and both physical and chemical processes involved in the Cu(II) removal; (3) Cation exchanges with H^+ from COOH and phenolic OH groups and with NH_4^+ from $–COONH_4$ were likely the primary mechanisms of Cu(II) chemisorption adsorption onto the poly(AA/CSP) as forms of Cu^{2+} and $CuOH^+$; (4) The equilibrium data were well fitted by the Langmuir isotherm with the maximum monolayer adsorption capacity of 200.3 mg/g; (5) The adsorption was a spontaneous and exothermic process co-driven by enthalpy and entropy.

Keywords: adsorption; chestnut shell; copper; hydrogel; melanin

Citation: Zhang, H.; Li, G.-W.; Feng, W.; Yao, Z.-Y. Cu(II) Adsorption from Aqueous Solution onto Poly(Acrylic Acid/Chestnut Shell Pigment) Hydrogel. *Water* **2022**, *14*, 3500. https://doi.org/10.3390/w14213500

Academic Editor: Efthimia A. Kaprara

Received: 12 October 2022
Accepted: 30 October 2022
Published: 2 November 2022

1. Introduction

Heavy metal pollution has become a global environmental issue and a significant concern due to the toxic, bio-accumulative, and non-degradable nature of heavy metals. Copper is the heavy metal used in electric appliances, pesticides, electroplates, and anti-fouling paints. Although it is an essential element for living beings, excessive copper intake may cause bio-accumulation, promote tissue peroxidation, and even lead to cancers [1]. Therefore, this heavy metal must be removed from aqueous effluents before discharge into water bodies. Thus, many techniques have been employed for heavy-metal removal from wastewater, such as ultrafiltration, reverse osmosis, coagulation, adsorption, electrodeposition, and chemical precipitation [2–6]. Among all of these strategies, adsorption is frequently applied for removal by taking advantage of its simple operation, high removal rate, low cost, and excellent renewability [7]. Adsorbents are the material basis of the adsorption technique; thus, developing novel adsorptive materials is a research focus of wastewater treatment. A great variety of materials, such as hydrogels [8], agricultural waste [4], and carbon materials [9], have been developed for heavy-metal adsorption. Among them, hydrogels are a kind of functional polymer feasible for removing heavy metals thanks to their three-dimensional network structure and abundant hydroxyl, amine, and carboxyl [10,11] hydrophilic groups. Such a structure and groups control the diffusion processes of water absorbing and heavy-metal binding [12]. Most hydrogels used in industrial and agricultural practices are made from fossil-based chemicals with high production costs and negative environmental effects. Currently, much attention is being

paid to introducing cheap, non-toxic, biodegradable, and renewable bio-based materials into hydrogel production.

Some biopolymers, such as starch, cellulose, and chitosan [13], have been employed to prepare hydrogels for heavy-metal adsorption [12]. However, the price and the heavy-metal-catching ability of the raw substrates should be considered for the high adsorption efficiency and cost performance of as-synthesized hydrogels. Biopolymers from abundant agro-wastes are thus a favorable option because they not only provide excellent water purification performance and cut the hydrogel fabrication cost, but also minimize the environmental impact of the agro-wastes.

Melanin is a pigmentary biopolymer oxidatively formed from phenolic or indolic monomers. It exists in all large taxa of prokaryotes and eukaryotes [14] and can be directly recovered from bio-wastes such as chestnut shells [15], apricot kernel skins [16], and olive mill waste [17]. Although the chemical structures of melanin in their natural state are still sealed, their high affinity for metal ions in vivo and in vitro has been well documented [18,19], presenting the potential for heavy-metal removal from wastewater.

Chestnut has always been a popular agricultural product, and its shells (pericarp and testa) are the chestnut-processing residue. Chestnut shell pigment (CSP) is herbal melanin isolated from the byproduct. The pigment is abundant in carboxyl, hydroxyl, and carbonyl [9], which have been identified as potential binding sites of metal ions [20,21]. Unfortunately, CSP is partially dissolved in water and therefore unable to be innately used as an adsorbent for wastewater treatment. Some technologies have been developed to overcome this limitation. Zhou et al. [22] crosslinked CSP with formaldehyde. Su et al. [23] prepared CSP/SiO_2 composite. Yao et al. [24] insolubilized CSP by thermal treatment. All of these CSP-based materials gave high adsorption efficiency for copper ions, showing the great potential of CSP to make adsorbents for Cu(II) removal.

In this study, the first effort was made to incorporate melanin, specifically CSP, into a hydrogel through polymerization with acrylic acid (AA) without using traditional crosslinkers, and the possible use of as-prepared hydrogel for Cu(II) adsorption from aqueous solutions was also investigated. To elucidate the physicochemical properties of the poly(AA/CSP), the samples were characterized by Fourier transform infrared spectroscopy (FT–IR) and a scanning electron microscopy (SEM). A batch method was used to examine the Cu(II) adsorption performance of the copolymer. In order to uncover the adsorption natures, parameters of equilibrium isotherm, kinetics, and thermodynamics were evaluated. Furthermore, the paper investigated the binding mechanisms of copper onto this biosorbent.

2. Materials and Methods

2.1. Materials

All the reagents were of analytical grade and were produced in China. Cupric nitrate was used to prepare the Cu(II) solutions, and nitric acid and sodium hydroxide were employed to adjust the pH of copper solutions. The fresh Chinese chestnuts (*Castanea mollissima* Blume) were bought from a market in Kunming, China.

2.2. CSP Preparation

The pigment was prepared according to the method of Zhou et al. [22], with slight modifications. Chestnut fruits were peeled manually, and the shells were crushed to less than 4 mm. The scraps were extracted twice with 0.2 mol/L NaOH aqueous solution at a liquid-solid ratio of 15 mL/g for 24 h at 50 °C. The crude pigment solution was achieved by filtration and acidified to pH 2 with concentrated HCl. The static settlement was conducted at ambient temperature for 24 h, and the precipitate was collected by centrifugation at 3500 rpm for 10 min. After being frozen at −80 °C for 12 h in a refrigerator, it was thawed at room temperature, centrifuged, washed twice with water of pH 3 adjusted with HCl, dried at 50 °C, sealed in a plastic bag, and stored at 4 °C.

2.3. Poly(AA/CSP) Synthesis

Specifically, 2.5 mL of AA, 25.6 mL of 0.59% (*w*/*w*) CSP solution in 1.32% (*w*/*w*) ammonium hydroxide, and 0.55 g of ammonium persulphate as an initiator, were successively introduced into a flask and heated in a water bath with a magnetic stirrer (DF-101T, Yuhua, Gongyi, China) at 500 rpm at 80 °C until the stirrer could not rotate due to the high viscosity. After being cooled to the ambient temperature with tap water, the gel was cut into strips about 5 mm in width and rinsed with 150 mL anhydrous ethanol four times, vacuum dried at 65 °C, crushed, and screened to collect 40 to 60 mesh particles for the adsorption measurement.

2.4. Poly(AA/CSP) Characterization

Fourier transform infrared spectroscopy (FT–IR) was used to identify the functional groups participating in the copper binding [5]. The FT–IR spectra were recorded on a Nicolet Avatar 380 spectrometer (Thermo Scientific, Waltham, MA, USA) after the samples were ground with KBr at a ratio of about 1:400 by weight and the mixture was pressed into transparent discs. Scanning Electron Microscopy (SEM) can reveal the microstructure of poly (AA/CSP). The sample was coated with a gold film before the morphology detection with a Hitachi 4800 scanning electron microscope (SEM; Hitachi, Tokyo, Japan). The pH point of zero charges (pH_{pzc}) was adopted to determine the solution pH at which the net charge of the poly(AA/CSP) surface is zero, and its value was measured by the immersion technique [25].

2.5. Adsorption Experiments

All adsorption experiments were carried out in a batch process. The adsorbent of 0.05 g was mixed with 50 mL copper solution of a given concentration and rotated on a thermal-controlled shaker (TS-211B TENSUC, Shanghai, China) at 120 rpm. To check the effects of pH on the adsorption, Cu(II) in 200 mg/L solutions with different initial pH values were used for the adsorption at 300 K for 24 h. In kinetic experiments, the copper solutions of pH 6 with various concentrations were shaken at 300 K for different contact times. For equilibrium data collection, the copper solutions of pH 6 with various concentrations were shaken for 24 h at different temperatures. After the adsorption, the suspension was filtered by a 0.45-μm microporous membrane on an injector. The residual copper concentration in the filtrate was measured by an AA-100 atomic absorption spectrophotometer (Perkin-Elmer Inc., Foster City, CA, USA). The copper adsorption quantity, q (mg/g), was calculated by Equation (1).

$$q = (C_0 - C)V/m \quad (1)$$

where C_0 (mg/L) and C (mg/L) are the Cu(II) concentrations in the aqueous phase before and after the adsorption, respectively, m (g) is the mass of sorbent, and V (L) is the solution volume.

All of the experiments were conducted in triplicate, and the arithmetic averages of the experimental data are presented. The nonlinear regressions were performed using the Solver tool of Microsoft® Excel 2016.

3. Results

3.1. Surface Morphology of Poly(AA/CSP)

The heavy-metal adsorption performance of hydrogels strongly depends on their surface properties and network structures. Therefore, we investigated the surface morphology of poly(AA/CSP) by SEM, and the typical images are shown in Figure 1. The surface is loose, coarse, and porous, with spindle-shaped bars randomly interconnected to form the disordered pores (Figure 1 insert).

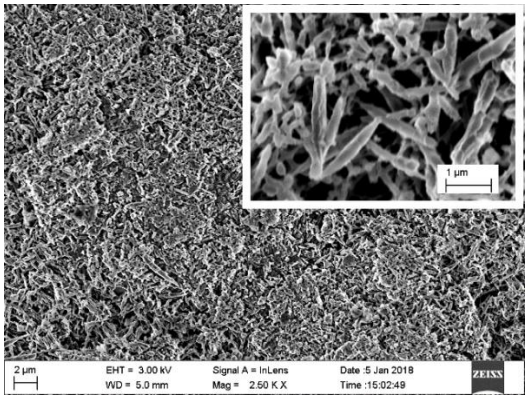

Figure 1. Scanning electron micrograph of poly(acrylic acid/chestnut shell pigment).

3.2. FT–IR of Poly(AA/CSP)

The FT–IR spectra of the native and the copper-loaded poly(AA/CSP) are shown in Figure 2. The absorption signals at 3600–3100 cm^{-1} corresponded to the stretching of O–H and N–H. In particular, the band at around 3143 cm^{-1} was attributed to N–H stretching from the ammonium ions [26]. The band at 804 cm^{-1} resulted from the out-of-plane bending vibrations of N–H [27]. The N–H groups came from three sources: (1) amino groups on CSP molecules; (2) NH_4^+ from the ammonium hydroxide solution used as a solvent for CSP and as a neutralizer for AA; and (3) NH_4^+ from the initiator of ammonium persulphate. These NH_4^+ ions formed salts with carboxyl and phenol groups and were retained in the hydrogel. The bands located at 1716, 1565, 1452, and 953 cm^{-1} resulted from carboxylic C=O stretching, COO^- asymmetric stretching, COO^- symmetric stretching, and O–H out-of-plane bending of COOH, respectively [28]. The band at 1169 cm^{-1} was related to the −C−OH stretching of phenol groups [29]. As shown in Figure 2, the copper adsorption decreased the intensities of these bands associated with NH, COOH, COO^-, and phenolic OH. The peaks centered at 1618 and 1402 cm^{-1} were assigned to the C=C stretching of aromatic rings and $-CH_2-$ deformation, respectively [30]. Some new bands presented in the spectrum of copper-loaded sample. The twin bands at 3550 and 3475 cm^{-1} could be associated with the O–H stretching of copper hydroxide cations, and the absorption at 484 cm^{-1} corresponded to the Cu–O stretching of the cations [2,31].

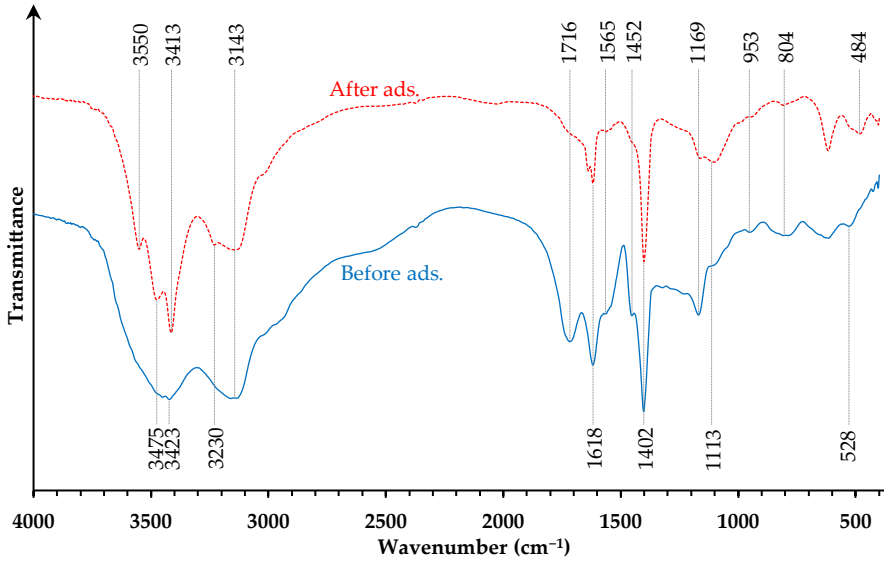

Figure 2. FT–IR spectra of poly(acrylic acid/chestnut shell pigment) before and after Cu(II) adsorption.

3.3. Effect of pH on Adsorption

The pH-dependent Cu(II)-adsorption behavior of the poly(AA/CSP) was studied, and the result is exhibited in Figure 3. The adsorption capability went up along with the pH increase and reached the maximum of 150.98 mg/g at pH 6. The authors haven't examined the adsorption over pH 6 due to $Cu(OH)_2$ precipitate formation. The pH_{pzc} was also determined and showed a value of 5.2.

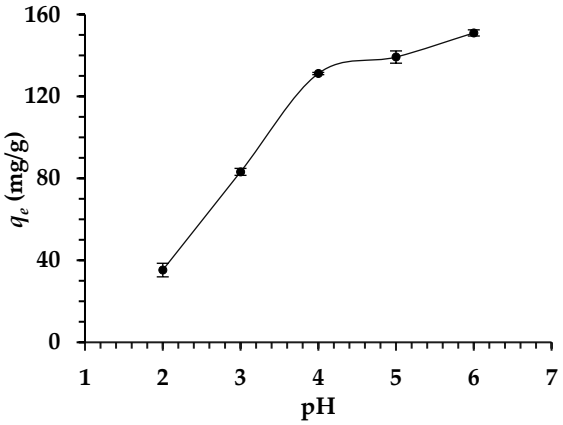

Figure 3. Effect of solution pH on Cu(II) adsorption onto poly(acrylic acid/chestnut shell pigment) (Temperature = 300 K, contact time = 24 h, adsorbent dosage = 1 g/L, initial concentration = 200 mg/L).

3.4. Adsorption Kinetics

The Cu(II) adsorption capacity onto the poly(AA/CSP) from the solutions with different initial concentrations was examined at a series of contact time. The adsorption process of Cu(II) onto the poly(AA/CSP) showed multiphasic kinetics (Figure 4). With the prolonged contact time, the adsorption capacity increased rapidly, slowed down, and finally reached the dynamic equilibrium. At all the tested concentrations, the adsorption equilibrium is reached within 720 min.

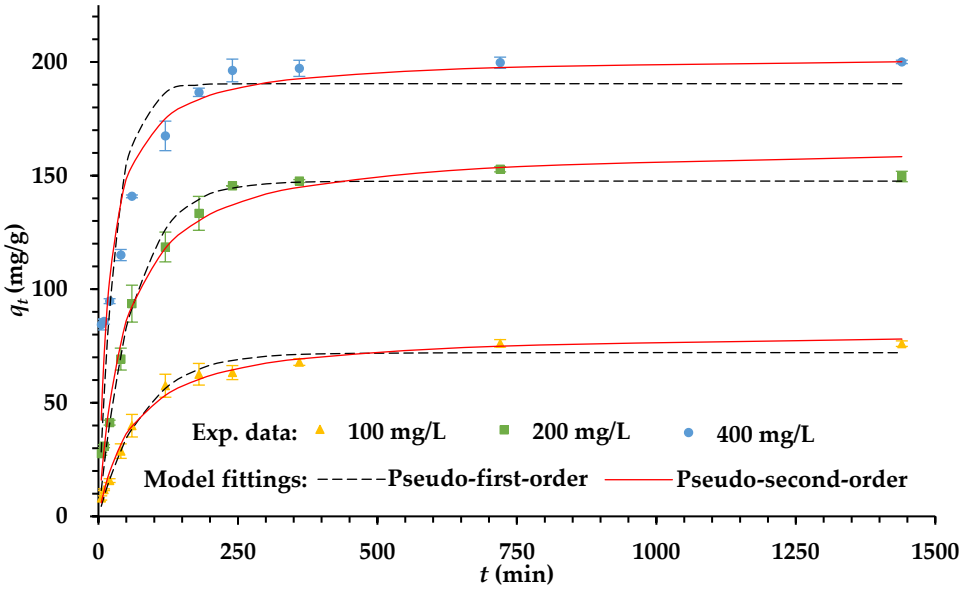

Figure 4. Adsorption kinetics of Cu(II) on to chestnut shells at different initial concentrations (acrylic acid/chestnut shell pigment) (Temperature = 300 K, pH = 6, adsorbent dosage = 1 g/L).

Kinetic modeling of sorption helps to predict the conditions under which the process can optimally work for a given system. The significant dependence of the instant adsorption

capacity on the contact time encouraged us to further fit the data with two famous kinetic models, i.e., the pseudo-first-order and pseudo-second-order equations.

The pseudo-first-order kinetic model [32] hypothesized that the elimination rate of adsorbate is proportional to the number of active sites available on an adsorbent. Equation (2) emphasizes that this model expresses the kinetic data in relation to the sorption rate and capacity:

$$q_t = q_e - q_e\, e^{-k_1\, t} \tag{2}$$

where q_e (mg/g) and q_t (mg/g) are the amounts of copper adsorbed at equilibrium and at time t (min), respectively; k_1 (1/min) is the adsorption rate constant.

The pseudo-second-order kinetic model [33] is based on the rate-limiting step of adsorption, which involves either electron sharing or electron transfer between adsorbate and adsorbent. The model is represented as

$$q_t = k_2\, {q_e}^2\, t/(1 + k_2\, q_e\, t) \tag{3}$$

where k_2 (g/mg/min) is the adsorption rate constant; q_e, q_t, and t are the same as the definitions in Equation (2).

The experimental data before adsorption equilibrium were nonlinearly fitted to both the kinetic equations, and the plots are shown in Figure 4. The parameters including k_1, k_2, and q_e are listed in Table 1. The results signify that both kinetic models sufficiently described the time course data, suggesting that both chemical and physical reactions occurred in the adsorption process.

Table 1. Kinetic parameters of Cu (II) adsorption onto poly(acrylic acid/chestnut shell pigment) at temperature = 300 K, pH = 6, and adsorbent dosage = 1 g/L.

C_0 (mg/L)	Pseudo-First Order			Pseudo-Second Order		
	q_e (mg/g)	K_1 (10^{-3}/min)	R^2	q_e (mg/g)	K_2 (10^{-4}g/mg/min)	R^2
100	72.04 ± 1.30	12.69 ± 2.29	0.9588	81.51 ± 1.61	1.931 ± 0.33	0.9631
200	147.5 ± 1.84	16.13 ± 1.61	0.9742	163.4 ± 2.17	1.182 ± 0.11	0.9692
400	190.4 ± 2.75	32.25 ± 2.41	0.8698	202.7 ± 3.33	2.682 ± 0.32	0.9088

3.5. Adsorption Equilibrium

Studies on equilibrium characteristics endeavor to understand the surface properties of adsorbents and the interaction between adsorbents and adsorbates. Two popular isotherms, the Langmuir and the Freundlich, were employed to describe the relationship between the copper amounts on the poly(AA/CSP) surface and in the liquid phase. The Langmuir isotherm model postulates monolayer adsorption onto the homogeneous surface with a fixed number of identical sites [34]. It is generally shown as the following equation:

$$q_e = q_m\, K_L\, C_e/(1 + K_L\, C_e) \tag{4}$$

where q_e (mg/g) and q_m (mg/g) are, respectively, the amount of copper adsorbed at equilibrium and the monolayer adsorption capacity of the adsorbent; K_L (L/mg) is the Langmuir constant giving information on the binding energy of adsorption process; C_e (mg/L) is the residual copper concentration of the solution at equilibrium.

The Freundlich model explains how adsorption takes place on a heterogeneous adsorbent surface by the interaction between the adsorbed molecules with the non-uniform sorption heat over the surface [35]. The model is expressed by the following equation:

$$q_e = K_F\, {C_e}^{1/n} \tag{5}$$

where q_e and C_e are defined as the same in Equation (5), and $1/n$ and K_F ($\mathrm{mg}^{1-1/\mathrm{n}/\mathrm{g}}/\mathrm{L}^{1/\mathrm{n}}$) are two empirical parameters of the adsorption intensity and capacity, respectively.

The nonlinear fitting results of the equilibrium data to the models are illustrated in Figure 5, and the isotherm parameters are given in Table 2. The experimental data points are closer to theoretical lines in the fitting plot of the Langmuir (Figure 5a) than in that of the Freundlich (Figure 5b), and the R^2-values for the Langmuir are greater than those for the Freundlich. These consequences indicate the better validity of the Langmuir model to describe the experimental data and ensure the monolayer copper formation on the surface of the polymers. The maximum monolayer adsorption capacity, q_m, was calculated to be 200.3 mg/g (Table 2), suggesting that the poly(AA/CSP) performed well for the adsorptive removal of copper ions from the water.

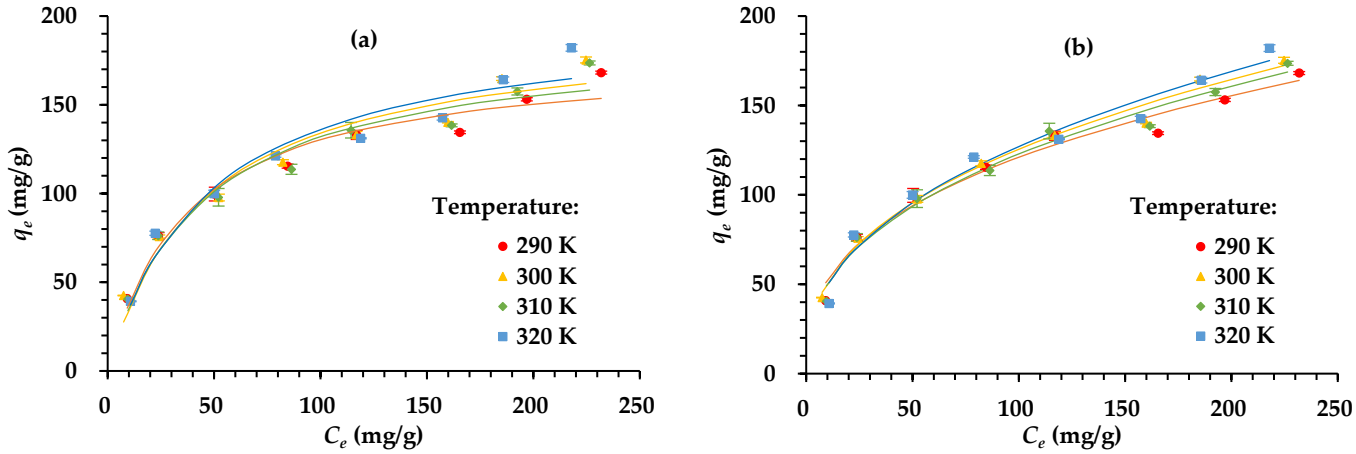

Figure 5. (**a**) Langmuir and (**b**) Freundlich isotherms for Cu(II) adsorption onto poly(acrylic acid/chestnut shell pigment) (Contact time = 24 h, pH = 6, adsorbent dosage = 1 g/L).

Table 2. Isotherm parameters of Cu(II) adsorption onto poly(acrylic acid/chestnut shell pigment) at contact time = 24 h, pH = 6, adsorbent dosage = 1 g/L.

T/K	Langmuir			Freundlich		
	q_m (mg/g)	K_L (L/g)	R^2	K_F ($mg^{1-1/n}/g \cdot L^{-1/n}$)	1/*n*	R^2
290	178.1 ± 0.71	27.08 ± 0.50	0.9609	22.76 ± 0.56	0.3626 ± 0.0034	0.9751
300	194.5 ± 1.88	22.12 ± 1.59	0.9509	20.67 ± 0.96	0.3916 ± 0.0071	0.9878
310	188.4 ± 2.94	23.18 ± 2.08	0.9540	20.45 ± 1.17	0.3892 ± 0.0163	0.9796
320	200.3 ± 2.75	21.27 ± 1.65	0.9484	19.16 ± 1.02	0.4110 ± 0.0093	0.9702

3.6. Adsorption Thermodynamics

In engineering practice, thermodynamics is an important aspect indicating the spontaneity, heat, and driving force of reactions. The thermodynamic parameters including the free energy change (ΔG°), the enthalpy change (ΔH°), and the entropy change (ΔS°) are related to an adsorption process changing along with temperatures, from which some adsorption mechanisms can be deduced [36]. The ΔG° (J/mol) directs whether a reaction is spontaneous. Its values depend on the thermodynamic equilibrium constant, *Kc*, and can be obtained from the equation:

$$\Delta G^\circ = -RT \ln Kc \quad (6)$$

where R (8.314 J/mol/K) is the universal gas constant, T (K) is the absolute temperature, and K_C equals the Langmuir constant, K_L, with the unit of L/mol. The ΔG° values calculated by Equation (7) are listed in Table 3.

Table 3. Thermodynamic parameters of Cu(II) adsorption onto poly(acrylic acid/chestnut shell pigment) at contact time = 24 h, pH = 6, adsorbent dosage = 1 g/L.

T (K)	ΔG° (kJ/mol)	ΔH° (kJ/mol)	ΔS° (J/mol·K)	R^2
290	-17.97 ± 0.04	-5.182	43.70	0.9878
300	-18.08 ± 0.02			
310	-18.81 ± 0.05			
320	-19.18 ± 0.02			

The ΔG° also relates to the ΔH° (J/mol) and the ΔS° (J/mol/K) by Equation (8):

$$\Delta G^\circ = \Delta H^\circ - T\,\Delta S^\circ \quad (7)$$

By this equation, the authors calculated ΔH° and ΔS° from the intercept and the slope of the straight line of ΔG° versus T (Figure 6), respectively, and their values are recorded in Table 3.

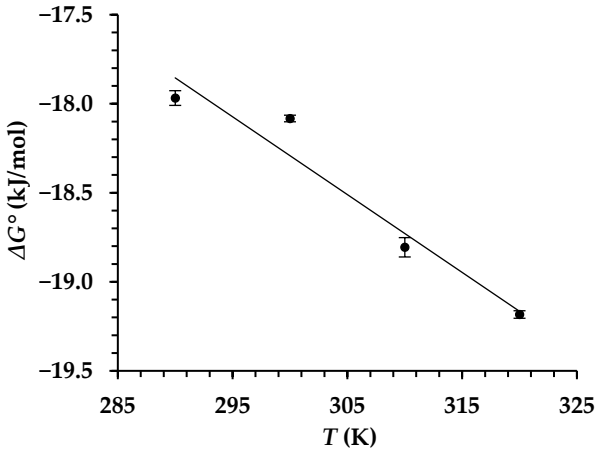

Figure 6. Thermodynamic plot for Cu(II) adsorption onto poly(acrylic acid/chestnut shell pigment) (Contact time = 24 h, pH = 6, adsorbent dosage = 1 g/L).

4. Discussion

4.1. Synthesis of Hydrogel Adsorbent

The hydrogel polymers made of anionic monomers can be used as adsorbents for cationic species such as heavy metal ions. Their swelling nature is favorable to capturing the adsorbates. Therefore, the polymers have been considered as adsorbent candidates. Polyacrylic-type hydrogels have the major market share of superabsorbents because of their simple synthesis, easy storage, and good performance for water-holding and heavy-metal scavenging. However, the raw materials of such polymers as AA and their derivatives are fossil chemicals, which are nonrenewable, costly, and hazardous to the environment. A strategy for overcoming these shortcomings, to some extent, is copolymerizing acrylic substances with natural polymers such as starch, cellulose, and lignin. For wastewater clean-up, the heavy-metal binding capability of the introduced bio-polymers should be taken into account because they might affect the performance of the copolymers. Melanin is well known as a strong binder for heavy metals both in vitro and in vivo [19,21]. However, to the best of our knowledge, melanin has not been used to synthesize hydrogels for heavy-metal adsorption so far. In this study, the melanin from chestnut shells was copolymerized with AA for the first time. Herein, the authors proposed the reaction for poly(AA/CSP) synthesis in Scheme 1.

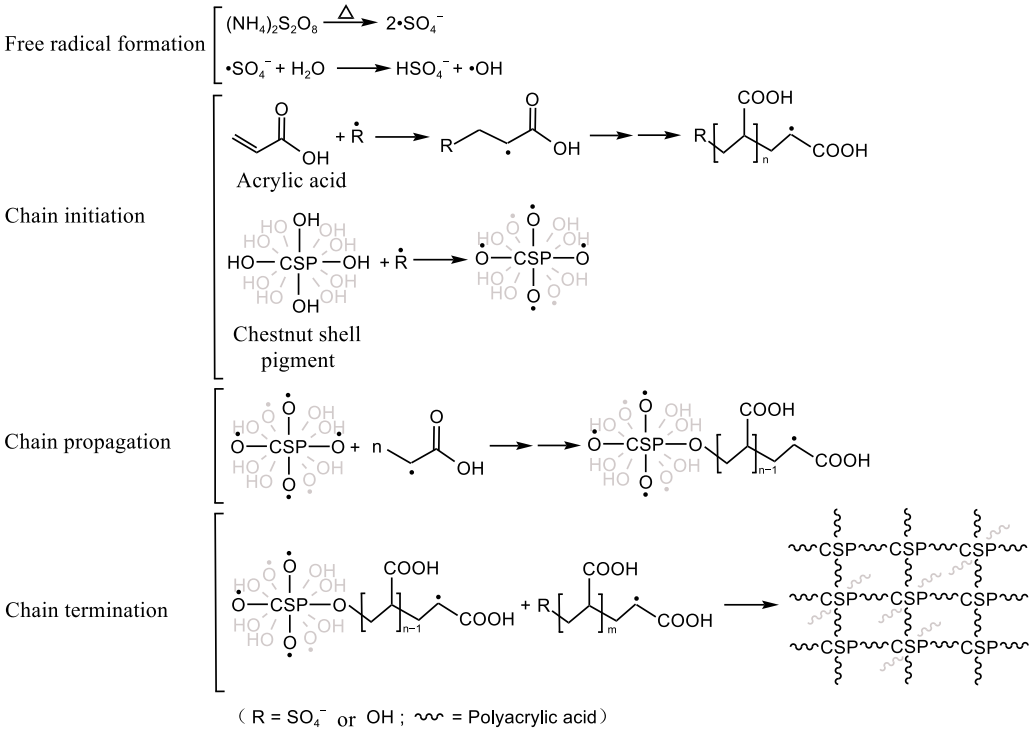

Scheme 1. Proposed reaction for synthesis of hydrogel crosslinked with chestnut shell pigment.

Ammonium persulphate was employed as the initiator, decomposing and generating sulfate anion radicals ($\cdot SO_4^-$) under heating. Some sulfate anion radicals despoiled hydrogen from water molecules, forming hydroxyl radicals (·OH). The sulfate anion and hydroxyl radicals attracted to the hydrogen from the functional groups, such as hydroxyl groups, on CSP, producing macroradicals of CSP, which initiated the polymerization of the AA to form the copolymer. Abundant functional groups on CSP radically react with the AA to form a three-dimensional structure, which rendered the copolymer stable in solutions and made it able to catch large quantities of copper ions.

In traditional polyacrylic-type superabsorbent preparation, *N*,*N*′-methylenebisacrylamide (MBA) is used as a crosslinker. Our preliminary experiments found that supplementing MBA made the network chains of poly(AA/CSP) less flexible and thus decreased the swelling and the Cu(II)-adsorbing capacities. Therefore, this reagent was not used. As shown in Scheme 1, CSP was attacked by $\cdot SO_4^-$ and ·OH to form molecules with multi-radicals and crosslinked polyacrylic acid chains to build 3D interconnected networks. In this sense, CSP worked as a crosslinker. CSP is a byproduct of the chestnut industry. It is cheap, abundant, renewable, easily available, and environmentally friendly. These qualities make the superabsorbent less expensive, more sustainable, and more environmentally benign to substitute MBA with CSP.

4.2. Adsorption Performance

Traditional acrylic-based hydrogels have fewer pores. Some researchers combined porous materials, such as kaolin [37], montmorillonite [38], and attapulgite [39], into the hydrogels to enhance their adsorption performance. Although such materials were not used in this study, the as-synthesized hydrogel shows a very developed porous structure, favoring Cu(II) diffusion, hydrogel swelling, and high copper adsorption. Its monolayer adsorption capacity of copper derived from the Langmuir isotherm (q_m) is 200.3 mg/g, higher than some earlier reported polyacrylic-type hydrogels such as poly(N-isopropylacrylamide-co-acrylic acid) (67.3 mg/g) [40], starch-g-poly(acrylic acid) (177.8 mg/g) [41], and acrylic-acid-co-acrylamide onto cellulose (82.07 mg/g) [42]. Melanin is a "trap" to inactivate toxic metals in living organisms [43]. Using melanin such as CSP as a crosslinker is a reasonable

choice to improve the heavy-metal adsorption performance of polyacrylic-type hydrogels. The q_m-value of poly(AA/CSP) is also higher than q_m-values for other CSP-based materials, such as formaldehyde crosslinked CSP (29.8 mg/g) [22], CSP/SiO_2 composite (18.9 mg/g) [23], and insolubilized CSP (33.2 mg/g) [24]. It is also higher than some recently reported adsorbents, such as Thiol-functionalized cellulose nanofiber membranes (49.0 mg/g) [43], sawdust chitosan nanocomposite beads (7.32 mg/g) [44], and corn silk (15.35 mg/g) [5]. The better performance indicates indicate that it is feasible to develop the poly(AA/CSP) for Cu(II) removal from water.

4.3. Adsorption Mechanisms

The kinetic data can be simulated by the pseudo-first-order and the pseudo-second-order models, suggesting the involvement of physical and chemical adsorption processes [45]. For the initial Cu(II) concentrations of 100 and 200 mg/L, the R^2-values were over 0.95 for both models. Such behavior may also be because the Cu(II) concentrations are not in the rate governing range. Compared to 100 and 200 mg/L, the initial Cu(II) concentrations of 400 mg/L gave lower R^2-values for the pseudo-first-order model (0.8698) and the pseudo-second-order (0.9088) model, as shown in Table 1, because of a mixed response of both of the models which cannot wholly fit the data alone [46].

Hydrogel swelling occurred in the Cu(II) adsorption process, made polymer chains formed flexible networks, increased the surface area of poly(AA/CSP), and allowed the copper ions to interact with binding sites in the hydrogel matrix. Furthermore, the electrostatic interaction between the poly(AA/CSP) surface and Cu(II) ions participated in the Cu(II) adsorption process. The adsorption capacity increased with the solution pH, and pH 6 was optimal. At a higher pH value, the adsorbent surface was more negatively and less positively charged, making the cationic copper more readily adsorbed. At the optimal pH, there were positive net charges on the adsorbent surface due to the pH_{pzc} of 5.2, and the electrostatic attraction presented as a driving force of the adsorption.

Ion exchange is involved in the chemical adsorption of Cu(II) onto poly(AA/CSP). Poly(acrylic acid) can adsorb cationic metals by the ionic exchange mechanism due to abundant carboxylic groups [47]. Melanin is a naturally occurring cation exchange material [48], and CSP has been reported as a cationic exchanger [2]. In this study, copper uptake reduced the absorbance at 3143 (N−H stretching of NH_4^+), 804 (out-of-plane bending vibrations of N–H), 1565 (COO^- asymmetric stretching), and 1452 cm^{-1} (COO^- symmetric stretching). This suggests an ion exchange between Cu(II) and NH_4^+ of –$COONH_4$. The copper addition also weakened the intensity of the peaks at 1716 (C=O stretching of COOH), 953 (O–H out-of-plane bending of COOH), and 1169 cm^{-1} (phenolic −C−OH stretching). Such changes suggest the involvement of COOH and phenolic OH groups in the Cu(II) binding through ion exchange between Cu(II) and H^+ from COOH or phenolic OH groups. The presence of the twin bands at 3550 and 3475 cm^{-1} (O–H stretching of copper hydroxide cations) as well as the absorption at 484 cm^{-1} (Cu–O stretching) gave an indication that some Cu(II) were bound on the hydrogel as copper hydroxide cations ($CuOH^+$) [2]. From the viewpoint of pH dependence of Cu(II) adsorption onto poly(AA/CSP), the excess of H^+ ions in the solution with a lower pH competed with the Cu(II) cations for ion-exchange with NH_4^+ ions. The H^+ ions also inhibited proton dissociation from the carboxylic and phenolic groups to ion-exchange with the Cu(II) cations. This also contributed to the better adsorption capacity at a higher pH. At the optimal pH of 6, Cu^{2+} dominated the Cu(II) species, and a small part of Cu(II) existed as $CuOH^+$ [49]. The participation of $CuOH^+$ in the adsorption was evidenced by FT–IR spectroscopy, as mentioned earlier.

The negative ΔG°-values (Table 3) at all tested temperatures propose the spontaneous nature of the adsorption. The negative ΔH°-value and the positive ΔS°-value suggest that the process was exothermic and co-driven by enthalpy and entropy.

5. Conclusions

A novel hydrogel, namely the poly(AA/CSP), was successfully synthesized from CSP and AA without using traditional crosslinkers. The poly(AA/CSP) was used for the Cu(II) adsorption from water. The hydrogel has a porous structure with networks of interconnected spindle-shaped bars. The optimal pH of the copper solutions is 6 for the adsorption. The kinetic adsorption behavior obeys the pseudo-first-order and the pseudo-second-order models. Both physical (hydrogel swelling and electrostatic interaction) and chemical processes were involved in the Cu(II) removal. Cation exchanges with H^+ from COOH and phenolic OH groups and with NH_4^+ from $-COONH_4$ were likely the primary mechanisms of Cu(II) chemisorption onto the poly(AA/CSP) as forms of Cu^{2+} and $CuOH^+$. The equilibrium adsorption data are well described by the Langmuir isotherm model, with a maximum adsorption capacity of 200.3 mg/g. Thermodynamically, the adsorption is spontaneous and exothermic, co-driven by enthalpy and entropy. The cheap bio-based component, the inexpensive synthesis, and the good performance endow poly(AA/CSP) with a promising potential for heavy-metal removal from aqueous solutions.

Author Contributions: Conceptualization, H.Z. and Z.-Y.Y.; methodology, G.-W.L. and Z.-Y.Y.; software, H.Z. and W.F.; formal analysis, G.-W.L. and H.Z.; writing, original draft preparation, H.Z. and G.-W.L.; writing, review and editing, H.Z., W.F. and Z.-Y.Y. All authors have read and agreed to the published version of the manuscript.

Funding: This research was financially supported by the National Natural Science Foundation of China (No. 31770673) and the Faculty Start-up Grant to Dr. Zeng-Yu Yao from Southwest Forestry University (No. 111822). The atomic absorption spectrophotometer was supplied by the Valuable Equipment Sharing Platform of Southwest Forestry University.

Institutional Review Board Statement: Not applicable.

Informed Consent Statement: Not applicable.

Data Availability Statement: Not applicable.

Conflicts of Interest: The authors declare that they have no conflicts of interest.

References

1. Yang, F.; Pei, R.; Zhang, Z.; Liao, J.; Yu, W.; Qiao, N.; Han, Q.; Li, Y.; Hu, L.; Guo, J. Copper induces oxidative stress and apoptosis through mitchondria-mediated pathway in chicken hepatocytes. *Toxicol. In Vitro* **2019**, *54*, 310–316. [CrossRef] [PubMed]
2. Fu, W.Q.; Wen, Y.; Tang, W.J.; Yao, Z.Y. Cu(II) removal from aqueous solution by ultrafiltration assisted with chestnut shell pigment. *Water Conserv. Sci. Eng.* 2022. [CrossRef]
3. Chen, Z.; Wei, W.; Chen, H.; Ni, B.J. Recent advances in waste-derived functional materials for wastewater remediation. *Eco-Environ. Health* **2022**, *1*, 86–104. [CrossRef]
4. Simić, M.; Petrović, J.; Šoštarić, T.; Ercegović, M.; Milojković, J.; Lopičić, Z.; Kojić, M. A Mechanism Assessment and Differences of Cadmium Adsorption on Raw and Alkali-Modified Agricultural Waste. *Processes* **2022**, *10*, 1957. [CrossRef]
5. Petrović, M.; Šoštarić, T.; Stojanović, M.; Petrović, J.; Mihajlović, M.; Ćosović, A.; Stanković, S. Mechanism of adsorption of Cu^{2+} and Zn^{2+} on the corn silk (*Zea mays* L.). *Ecol. Eng.* **2017**, *99*, 83–90. [CrossRef]
6. Chen, Z.; Wei, W.; Zou, W.; Li, J.; Zheng, R.; Wei, W.; Ni, B.J.; Chen, H. Integrating electrodeposition with electrolysis for closed-loop resource utilization of battery industrial wastewater. *Green Chem.* **2022**, *24*, 3208–3217. [CrossRef]
7. Bolisetty, S.; Peydayesh, M.; Mezzenga, R. Sustainable technologies for water purification from heavy metals: Review and analysis. *Chem. Soc. Rev.* **2019**, *48*, 463–487. [CrossRef]
8. Burakov, A.E.; Galunin, E.V.; Burakova, I.V.; Kucherova, A.E.; Agarwal, S.; Tkachev, A.G.; Gupta, V.K. Adsorption of heavy metals on conventional and nanostructured materials for wastewater treatment purposes: A review. *Ecotoxicol. Environ. Saf.* **2018**, *148*, 702–712. [CrossRef]
9. Chen, Z.; Wei, W.; Ni, B.J.; Chen, H. Plastic wastes derived carbon materials for green energy and sustainable environmental applications. *Environ. Funct. Mater.* **2022**, *1*, 34–48. [CrossRef]
10. Wang, H.Q.; Xu, W.L.; Song, S.S.; Feng, L.; Song, A.X.; Hao, J.C. Hydrogels facilitated by monovalent cations and their use as efficient dye adsorbents. *J. Phys. Chem. B* **2014**, *118*, 4693–4701. [CrossRef]
11. Kaşgöz, H.; Durmuş, A.; Kaşgöz, A. Enhanced swelling and adsorption properties of AAm-AMPSNa/clay hydrogel nanocomposites for heavy metal ion removal. *Polym. Adv. Technol.* **2008**, *19*, 213–220. [CrossRef]
12. Khan, M.; Lo, I.M. A holistic review of hydrogel applications in the adsorptive removal of aqueous pollutants: Recent progress, challenges, and perspectives. *Water Res.* **2016**, *106*, 259–271. [CrossRef] [PubMed]

13. Hu, D.L.; Lian, Z.W.; Xian, H.Y.; Jiang, R.; Wang, N.; Weng, Y.Y.; Peng, X.W.; Wang, S.M.; Ouya, X.K. Adsorption of Pb(II) from aqueous solution by polyacrylic acid grafted magnetic chitosan nanocomposite. *Int. J. Biol. Macromol.* **2019**, *154*, 1537–1547. [CrossRef]
14. Benamer, S.; Mahlous, M.; Tahtat, D.; Nacer-Khodja, A.; Arabi, M.; Lounici, H.; Mameri, N. Radiation synthesis of chitosan beads grafted with acrylic acid for metal ions sorption. *Radiat. Phys. Chem.* **2011**, *80*, 1391–1397. [CrossRef]
15. Yao, Z.Y.; Qi, J.H.; Wang, L.H. Isolation, fractionation and characterization of melanin-like pigments from chestnut (*Castanea mollissima*) shells. *J. Food Sci.* **2012**, *77*, C671–C676. [CrossRef]
16. Li, H.J.; Li, J.X.; Zhao, Z. Characterization of melanin extracted from apricot (*Armeniaca sibirica*) and its effect on hydrazine-induced rat hepatic injury. *Sci. Asia.* **2016**, *42*, 382–391. [CrossRef]
17. Khemakhem, M.; Papadimitriou, V.; Sotiroudis, G.; Zoumpoulakis, P.; Arbez-Gindre, C.; Bouzouita, N.; Sotiroudis, T.G. Melanin and humic acid-like polymer complex from olive mill waste waters. Part I. Isolation and characterization. *Food Chem.* **2016**, *203*, 540–547.
18. Chen, S.G.; Xue, C.H.; Wang, J.F.; Feng, H.; Wang, Y.M.; Ma, Q.; Wang, D.F. Adsorption of Pb (II) and Cd (II) by squid *Ommastrephes bartrami* melanin. *Bioinorg. Chem. Appl.* **2009**, *2009*, 901563. [CrossRef]
19. Thaira, H.; Raval, K.; Manirethan, V.; Balakrishnan, R.M. Melanin nano-pigments for heavy metal remediation from water. *Sep. Sci. Technol.* **2018**, *54*, 265–274. [CrossRef]
20. Zdybel, M.; Chodurek, E.; Pilawa, B. Free radicals in ultraviolet irradiated melanins and melanin complexes with Cd (II) and Cu (II)–EPR examination. *J. Appl. Biomed.* **2015**, *13*, 131–141. [CrossRef]
21. Hong, L.; Simon, J.D. Current understanding of the binding sites, capacity, affinity, and biological significance of metals in melanin. *J. Appl. Biomed. B* **2007**, *111*, 7938–7947. [CrossRef] [PubMed]
22. Zhou, M.; Su, P.; Qi, J.H.; Hu, Y.; Yao, Z.Y. Double-catalyzed base-acid synthesis of chestnut shell pigment resin cross-linked with formaldehyde. *Appl. Mech. Mater.* **2014**, *587*, 663–668. [CrossRef]
23. Su, P.; Zhou, M.; Qi, J.H.; Kan, H.; Yao, Z.Y. Synthesis and copper sorption of chestnut-shell-pigment/SiO_2 composite. *Adv. Mater. Res.* **2014**, *1035*, 53–57. [CrossRef]
24. Yao, Z.Y.; Qi, J.H.; Hu, Y.; Wang, Y. Insolubilization of chestnut shell pigment for Cu (II) adsorption from water. *Molecules* **2016**, *21*, 405. [CrossRef]
25. Fiol, N.; Villaescusa, I. Determination of sorbent point zero charge: Usefulness in sorption studies. *Environ. Chem. Lett.* **2009**, *7*, 79–84. [CrossRef]
26. Ahmad, N.H.; Isa, M.I.N. Structural and ionic conductivity studies of CMC based polymerelectrolyte doped with NH_4Cl. *Adv. Mater. Res.* **2015**, *1107*, 247–252. [CrossRef]
27. Centeno, S.A.; Shamir, J. Surface enhanced Raman scattering (SERS) and FTIR characterization of the sepia melanin pigment used in works of art. *J. Mol. Struct.* **2008**, *873*, 149–159. [CrossRef]
28. Yu, Y.; Peng, R.; Yang, C.; Tang, Y. Eco-friendly and cost-effective superabsorbent sodium polyacrylate composites for environmental remediation. *Asian J. Mater. Sci.* **2015**, *50*, 5799–5808. [CrossRef]
29. de Oliveira, L.K.; Molina, E.F.; Moura, A.L.A.; de Faria, E.H.; Ciuffi, K.J. Synthesis, Characterization, and Environmental Applications of Hybrid Materials Based on Humic Acid Obtained by the Sol–Gel Route. *ACS Appl. Mater. Interfaces* **2016**, *8*, 1478–1485. [CrossRef]
30. Wander, M.M.; Bidart, M.G. Tillage practice influences on the physical protection, bioavailability and composition of particulate organic matter. *Biol. Fertil. Soils* **2000**, *32*, 360–367. [CrossRef]
31. Fu, J.L.; Liu, X.D.; Liu, L.; Meng, H.M.; Wang, X.B. Infrared and Raman spectral analysis of the polycrystalline copper hydroxonitrates. *IOP Conf. Ser. Mater. Sci. Eng.* **2020**, *774*, 012060. [CrossRef]
32. Lagergren, S. About theory of so-called adsorption of soluble substances. *K. Sven. Vetenskapsakad. Handl.* **1898**, *24*, 1–39.
33. Ho, Y.S.; McKay, G. Kinetic models for the sorption of dye from aqueous solution by wood. *Trans. IChemE Part B* **1998**, *76*, 183–191. [CrossRef]
34. Langmuir, I. The adsorption of gases on plane surfaces of glass, mica and platinum. *J. Am. Chem. Soc.* **1918**, *40*, 1361–1403. [CrossRef]
35. Freundlich, H.M.A. Concerning adsorption in solutions. *J. Chem. Phys.* **1906**, *57*, 385–470.
36. Dawood, S.; Sen, T.K.; Phan, C. Synthesis and characterisation of novel-activated carbon from waste biomass pine cone and its application in the removal of Congo red dye from aqueous solution by adsorption. *Water Air Soil Poll.* **2014**, *225*, 1818. [CrossRef]
37. Shen, S.H.; Zhang, Y.Y.; Li, T.B.; Zeng, Q.L. Preparation and water absorbency of superabsorbent kaolin/PAA-AM composite. *Adv. Mater. Res.* **2013**, *2203*, 1968–1976. [CrossRef]
38. Zhang, J.P.; Wang, L.; Wang, A.Q. Preparation and properties of chitosan-g-poly (acrylic acid)/montmorillonite superabsorbent nanocomposite via in situ intercalative polymerization. *Ind. Eng. Chem. Res.* **2007**, *46*, 2497–2502. [CrossRef]
39. Li, A.; Wang, A.Q.; Chen, J.M. Studies on poly (acrylic acid)/attapulgite superabsorbent composite. I. Synthesis and characterization. *J. Appl. Polym. Sci.* **2004**, *92*, 1596–1603. [CrossRef]
40. Chen, J.J.; Ahmad, A.L.; Ooi, B.S. Poly (N-isopropylacrylamide-co-acrylic acid) hydrogels for copper ion adsorption: Equilibrium isotherms, kinetic and thermodynamic studies. *J. Environ. Chem. Eng.* **2013**, *1*, 339–348. [CrossRef]
41. Zheng, Y.A.; Hua, S.B.; Wang, A.Q. Adsorption behavior of Cu^{2+} from aqueous solutions onto starch-g-poly (acrylic acid)/sodium humate hydrogels. *Desalination* **2010**, *263*, 170–175. [CrossRef]

42. Zhao, B.X.; Wang, P.; Zheng, T.; Chen, C.Y.; Shu, J. Preparation and adsorption performance of a cellulosic-adsorbent resin for copper (II). *J. Appl. Polym. Sci.* **2006**, *99*, 2951–2956.
43. Choi, H.Y.; Bae, J.H.; Hasegawa, Y.; An, S.; Kim, I.S.; Lee, H.; Kim, M. Thiol-functionalized cellulose nanofiber membranes for the effective adsorption of heavy metal ions in water. *Carbohydr. Polym.* **2020**, *234*, 115881. [CrossRef] [PubMed]
44. Kayalvizhi, K.; Alhaji, N.M.I.; Saravanakkumar, D.; Mohamed, S.B.; Kaviyarasu, K.; Ayeshamariam, A.; AlMohaimeed, A.M.; AbdelGawwad, M.R.; Elshikh, M.S. Adsorption of copper and nickel by using sawdust chitosan nanocomposite beads—A kinetic and thermodynamic study. *Environ. Res.* **2022**, *203*, 111814. [CrossRef]
45. He, H.C.; Huang, Y.B.; Yan, M.M.; Xie, Y.T.; Li, Y. Synergistic effect of electrostatic adsorption and ion exchange for efficient removal of nitrate. *Colloids Surf. A* **2020**, *584*, 123973. [CrossRef]
46. Singh, A.; Kumar, D.; Gaur, J.P. Removal of Cu(II) and Pb(II) by *Pithophora oedogonia*: Sorption, desorption and repeated use of the biomass. *J. Hazard. Mater.* **2008**, *152*, 1011–1019. [CrossRef]
47. Mohammadzadeh Pakdel, P.; Peighambardoust, S.J. A review on acrylic based hydrogels and their applications in wastewater treatment. *J. Environ. Manag.* **2018**, *217*, 123–143. [CrossRef]
48. White, L.P. Melanin: A naturally occurring cation exchange material. *Nature* **1958**, *182*, 1427–1428. [CrossRef]
49. Mensah, J.B.; Delidovich, I.; Hausoul, P.J.C.; Weisgerber, L.; Schrader, W.; Palkovits, R. Mechanistic studies of the $Cu(OH)^{+}$-catalyzed isomerization of glucose into fructose in water. *Chemsuschem* **2018**, *11*, 2579–2586. [CrossRef]